Measurement of Intrinsic Mechanical Loss in Aluminum Films from 3 to 25 GHz by HBAR Spectroscopy

Zachary Schaffer, Ahmed Hassanien, Mohammad Ayaz Masud, Gianluca Piazza
Department of Electrical and Computer Engineering
Carnegie Mellon University
Pittsburgh, PA
zschaffer@cmu.edu

Abstract-In this work we measure, for the first time, mechanical loss in an Al thin film from 3 GHz to 25 GHz through the use of high overtone bulk acoustic resonator (HBAR) spectroscopy. This is made possible by scaling down a HBAR to use a thin (200 nm) aluminum nitride (AlN) piezoelectric transducer and replacement of the thick substrate with a sputtered, suspended metal film (~1 µm). Resonant overtones are transduced piezoelectrically while >90% of the mechanical energy is confined to the Al, allowing Al mechanical loss to be accurately determined from quality factor at series resonance (Qs). Measured Qs for 7 overtones ranging from 3-25 GHz with values from 140 to 50 was found to be ~30% less than predicted by analytical models considering thermoelastic and phonon phonon damping. Additionally, measured frequency dependence of Q (f^{-0.46}) aligned well with the dependence predicted by thermoelastic and Landau Rumer regime phonon phonon damping (f-0.56) and was well above the f-1 dependence predicted by thermoelastic and Akhiezer regime phonon phonon damping. This technique can be applied to measure mechanical loss in metal thin films up to K band, allowing loss characterization and enabling informed decision making for design of many high frequency acoustic devices.

Keywords—high overtone bulk acoustic resonator (HBAR), quality factor, phonon loss, aluminum, mmWave, acoustic resonator

I. INTRODUCTION

Acoustic resonators are rapidly gaining interest as an approach to filtering throughout the K bands and above [1]. For filter applications resonator quality factor (Q) directly sets insertion loss, a key metric of filter performance. Current demonstrations of acoustic resonators operating in K through V bands do not have the performance necessary to compete with EM cavity or low temperature co-fired ceramic (LTCC) filter approaches. Significant challenges related to downscaling of film thickness and management of ohmic loss from device electrodes cause device frequency scaling to result in an increase of mechanical energy in the electrodes. As mechanical energy in the electrodes becomes more significant, mechanical loss in these layers begins to dominate resonator mechanical Q. Additionally, resonant modes well suited to K band such as thickness overmodes [2], and lateral or two dimensional plate modes are able to use low acoustic impedance (Z) metals such

as Al not attractive for the fundamental thickness mode resonators used for sub 6 GHz designs.

Ultrasonic attenuation in metals and other thin films has been studied, individual loss mechanisms identified, and analytical loss models quantified [3]. However, experimental results are limited, with minimal metal thin film measurements above 3 GHz. Mechanical loss is driven by a combination of thermoelastic damping (TED), phonon phonon (PP) interactions, as well as defect, interface and grain boundary scattering. At sub 3 GHz frequencies—where prior work has extracted loss experimentally—PP damping operates in the Akhiezer regime resulting in a constant fQ product. However, at higher frequency PP damping transitions to the Landau Rumer regime where quantized interactions of individual phonons dominate, and PP damping has a frequency independent Q.

Mechanical Q from ~1.5-3 GHz has been measured in suspended Al and W thin films using laser ultrasound transduction [4], [5]. This approach introduces minimal inaccuracy from the transduction method compared to piezoelectric approaches but requires a specific metal thickness per frequency and an optical measurement setup. Piezoelectric based transduction approaches can often measure loss at a range of frequencies from a single film thickness and can be measured electrically with a Vector Network Analyzer (VNA) and probes. These approaches rely on exciting either a resonant mode or operating using a pulse echo technique [6] to determine mechanical loss from a measured electrical response transduced by the piezoelectric layer. High overtone bulk acoustic resonators (HBARs) typically consist of a thin transducer and thick substrate. They have been used to accurately characterize loss in thick substrates for a number of single crystal materials including diamond up to 40 GHz [7]. Piezoelectric [8] and metal thin films have also been measured where the target layer makes up a small portion of the HBAR stack with a recent study on molybdenum measuring up to 20 GHz [9], [10]. However, in this approach accurate loss extraction can be difficult since loss in the other layers must be accounted for. This is further complicated as mechanical energy distribution in each overtone is not the same due to cutoff frequency trapping effects in the thickness direction [11] and lateral leakage from dispersion as well as unwanted excitation of lamb and surface acoustic wave spurious modes

[12]. When the material of interest makes up only a small portion of the HBAR loss, small but unaccounted for loss mechanisms produce large uncertainty.

We scale down HBAR thickness so that the bulk substrate is replaced by a relatively thin (~1 µm) suspended metal film as shown in Fig. 1. This allows for good confinement of mechanical energy to the layer of interest, reducing measurement uncertainty. Additionally, scaling down total thickness allows a lower overtone vs. frequency, enabling strong electrical response at high frequency. Device fabrication is made possible by the use of a through wafer etch process in which devices are released from the backside and measured as series pairs with the backside electrode left floating. We demonstrate this approach using an Al film and an AlN transducer. Measured Qs varied from 140 to 50 for 7 overtones ranging from 3 GHz to 25 GHz. These values were found to be ~25% less than predicted by analytical models considering TED and PP damping. Additionally, measured frequency dependence of Q ($f^{0.46}$) aligned well with the dependence predicted by TED and Landau Rumer regime PP damping models ($f^{0.56}$) and was well above the f^{-1} dependence predicted by TED and Akhiezer regime PP damping.

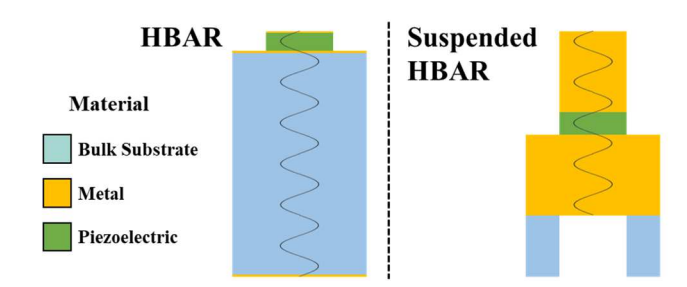


Fig. 1. Cross section of standard and suspended high overtone bulk acoustic resonator (HBAR), overlayed with stress distribution in the acoustic cavity. Note the larger portion of stack, and therefore larger percentage of mechanical energy present in the metal layer for the suspended HBAR design.

II. DESIGN

A. Principle of Operation

HBARs function by exciting a high overtone mode through both a thin piezoelectric transducer and thick material—typically a bulk substrate. By making the substrate much thicker than the piezoelectric transducer mechanical energy is confined mainly in the substrate causing mechanical loss in the resonant mode to be dominated by the Q of the substrate instead of the piezoelectric transducer. Mechanical loss in the substrate material can then be measured electrically from the Q of the transduced resonant modes. For these devices there are overtones with similar coupling over a wide frequency range, allowing Q to be measured for a range of frequencies from a single device.

The key challenges are having strong enough electrical transduction to accurately extract Q from electrical measurements and managing other loss mechanisms so that extracted Q corresponds to the mechanical loss of the layer of interest. In order to have accurate electrical measurements, the k_t^2 -Q product of each mode must be kept high and other

device parasitics must be minimized. In order to accurately extract material mechanical Q, the material of interest must dominate the Q of the stack or other loss mechanisms must be accurately de-embedded. The second approach is challenging, and the first creates a design tradeoff as the transducer and material of interest layer thickness must be sized to balance device k_t^2 and mechanical energy confinement. Extrinsic loss mechanisms also need to be managed, otherwise the measured Q of the mode will not be set by intrinsic material damping. Energy lost to lateral acoustic propagation beyond the active region of the resonator—anchor losses—can be managed with device area and shape, as this loss has some dependence on area to perimeter ratio. Ohmic loss from electrodes and interconnects can be managed by keeping the metal thick and minimizing routing.

B. Device Design

We use a HBAR stack consisting of a bottom electrode with 220 nm Al followed by a 10 nm Cr adhesion layer and 50 nm Pt seed for AlN growth, then a 200 nm AlN piezoelectric layer, and ultimately a 900 nm Al top electrode. Mechanical energy distribution as determined by finite element analysis indicates >90% of mechanical energy is confined to the Al layer. This is higher than the 80% value that could be estimated using the percentage Al thickness in the stack due to the low acoustic impedance of Al compared to AlN, Pt, and Cr. Our fabrication approach does not allow contact to the backside electrode, so a pair of series resonators are used. EM simulations using Ansys HFSS were used to determine the impact of ohmic loss. Due to the low k_t^2 -Q product of Al HBARs, high electrical conductivity of Al, and thick electrodes ohmic loss was simulated to be 1-3% loading on Qs over the 200 to 4000 µm² devices measured. Series resonance quality factor is used due to uncertainty in dielectric loss for our AlN film, and possible lateral leakage due to spurious modes near the antiresonance frequency.

C. Mechanical Quality Factor

For metal thin films thermoelastic damping (TED), phonon phonon (PP) damping, as well as scattering losses from defects, grain boundaries and roughness are relevant. TED is caused by irreversible heat flow along thermal gradients in a resonator generated by local expansion/contraction from acoustic vibrations. TED therefore has frequency dependence where loss worsens as long as vibrations are slower than heat transfer, but improves once vibrations surpass heat transfer speeds. Based on analytical modeling, we are still operating at lower frequency than the point of improvement. PP damping is modeled in the Akhiezer regime when resonant wavelength (λ) is significantly larger than the phonon mean free path, where the acoustic wave interacts with a range of thermal phonons causing local disturbances, and O is inversely proportional to frequency [13]. However, when λ is much less than the phonon mean free path PP interactions are described by the Landau-Rumer regime, where interactions occur between acoustic quanta and individual phonons. In this case interactions are local and Q is not dependent on frequency [14]. This means as frequency scales up, Q from phononphonon damping becomes fixed. Fig. 2. Shows analytical loss models and resultant *Q* vs frequency.

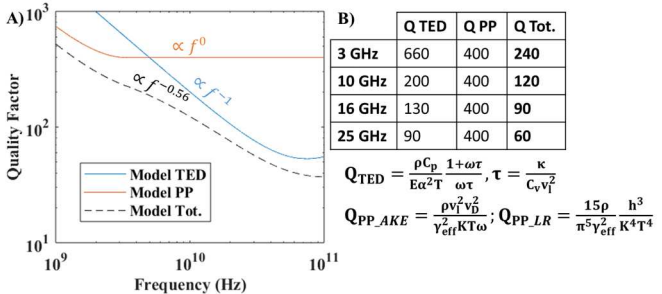


Fig. 2. A) Graph of Q due to thermoelastic damping (TED), phonon phonon (PP) damping. B) Calculated Q at specific frequencies and analytical loss models where: ρ is mass density, C_p is specific heat capacity at constant pressure, E is Young's modulus, α is thermal expansion coefficient, ω is angular frequency, κ is thermal conductivity, C_v is specific heat capacity at constant volume, v_l is longitudinal acoustic velocity, v_D is Debeye velocity, v_{eff} is effective Grüneisen parameter, K is Boltzmann constant, h is Planck's constant, m_e is electron mass, ϵ_F is Fermi energy, and σ_e is electrical conductivity.

Finally, film microstructure elements such as grain boundaries, defects and porosity, as well as surface roughness can cause additional scattering. Modeling these effects is complicated [15], and ultimately requires detailed information on film microstructure. For sputtered thin films, this microstructure is heavily dependent on deposition conditions and prior Al metal thin film measurements have shown a >4X reduction in Al Q at 1 GHz between magnetron sputtering and thermal evaporation techniques [9] indicating film microstructure may dominate Q in the specific films.

III. DEMONSTRATION

A. Fabrication

While this work reports Al HBARs, this technique can be applied to other metal thin films by replacing the Al with the metal of interest. Fabrication consists of a 4 step 2 mask process. (1) Starting from a high resistivity Si wafer, a bottom electrode stack consisting of 220 nm Al, 10 nm Cr, then 50 nm Pt is sputter deposited and patterned by ion milling. This stack is chosen so that AIN has a Pt seed for optimal growth, resistivity is low enough ohmic loss is manageable, and the Si interface is protected by Al for eventual backside release by DRIE. (2) This is followed by deposition of 200 nm AlN. (3) 900 nm of Al is then sputter deposited forming the top electrode. Efforts were taken to minimize film defects and roughness using a high power, low chamber pressure deposition condition. The top electrode film is ion milled using a 2 step process proposed by [16] where the first third of the total etch is milled at a shallow 45° angle and the final two thirds at a sharp 5° angle to prevent redeposition of material in the trench between series top electrodes. (4) A DRIE process with a 10 µm photoresist mask was then used to etch release holes from the backside of 500 µm Si wafer, stopping just before the Al seed layer of the bottom electrode. Aligning to wafer backside proved challenging so devices were released at the die level. Since the DRIE etch was deeper than our profilometer could measure, progress was tracked using focal

plane of an optical microscope. By comparing the focus position on either the Si backside or bottom of trench etch depth could be measured. Al is very resistant to DRIE so was not damaged by over etching, which was necessary to clear all Si from the active area underside. Fig. 3 shows images of fabricated devices.

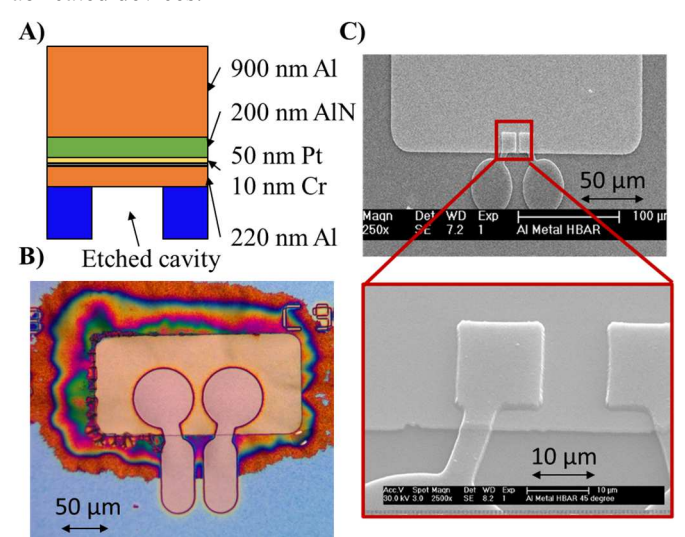


Fig. 3. A) Labeled device cross section. B) Optical image of released device. C) SEM image of unreleased device with inset focusing on active region.

B. Results

Measurements were carried out using a single 50 μ m pitch GS probe on an Agilent PNA-X. An off chip Short Open Load (SOL) calibration was run to extend the reference frame to the probe tips. On chip short structures were used to remove interconnect inductance to remove an electrical resonant mode from device capacitance and parasitic inductance. Admittance measurements were then fit to a multi branch mBVD model to extract per mode k_t^2 and Qs for each device. Fig. 4. shows response and extracted values for a characteristic device.

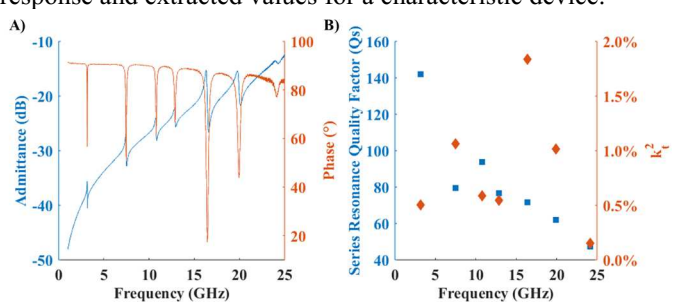


Fig. 4. A) Measured electrical response for 2500 μ m² device. B) Fit k_t^2 and Qs values for 2500 μ m² device.

In order to determine the impact of anchor loss, different shape and area devices were compared. Devices with square, circle, and pentagon shaped active regions did not significantly differ in response, so square devices were used to minimize ohmic loss as they can be packed closer. Response from devices with areas ranging from 200 to 4000 µm² are shown in Fig. 5. *Qs* remains relative constant over this wide range of areas, especially at higher frequencies, indicating

anchor loss is not a significant contributor to Q for the frequency range of interest.

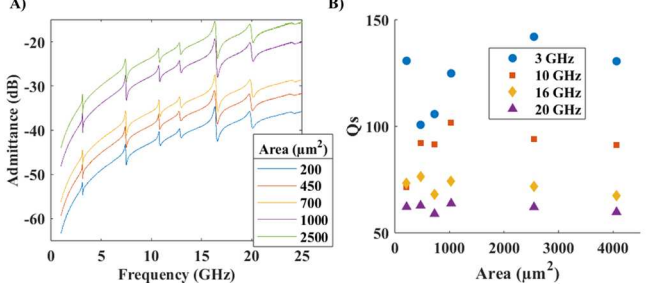


Fig. 5. A) Overlay of electrical response for 200 to 4000 μm² devices. B) Quality factor at series resonance (*Os*) vs device area for 3-20 GHz.

 k_t^2 and resonant frequency of the 7 measurable overtones for all area devices matches reasonably to FEA with discrepancy likely due to film thickness and material property errors. Measured Q values are ~25% below that predicted by analytical models, which considering the uncertainty of thin film properties such as thermal conductivity and Gruneisen parameter and wide experimental range depending on deposition quality represents good alignment. As seen in Fig. 6. the Q range for devices over a 20X area range is minor compared to frequency dependence. Additionally measured frequency dependence of Q of $f^{0.46}$ is close to the $f^{0.56}$ dependence predicted considering TED and Landau Rumer regime PP damping, and much higher than the f^{1} dependence predicted by TED and Akhiezer regime PP damping.

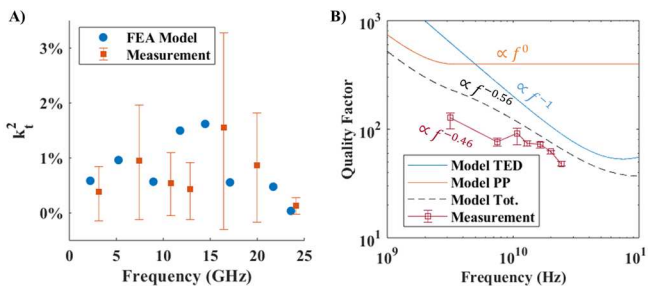


Fig. 6. A) Overlay of modeled and measured k_t^2 and resonant frequency of 200 to 4000 μm^2 devices with data points indicating median, and error bars indicating minimum and maximum measurements. B) Overlay of modeled Q from individual loss mechanisms, total modeled Q, and measured Q of 200 to 4000 μm^2 devices with data points indicating median, and error bars indicating minimum and maximum measurements.

IV. CONCLUSION

In this work we experimentally measured mechanical loss of thin film Al from 3 GHz to 25 GHz. Unlike typical HBARs, a suspended device with relatively thick Al and thin piezoelectric transducer is used to transduce overmodes with device Q set by mechanical loss in the metal layer. Over the 3-25 GHz frequency range Q decreased from 150 to 50 corresponding to an approximate 25% reduction from analytical models considering TED and Landau Rumer regime phonon phonon damping. The measured frequency dependence of Q of $f^{0.46}$ also corresponded well to the theory of $f^{0.56}$ and was far above the f^1 predicted by TED and Akhiezer regime phonon phonon damping. Characterization of

metal mechanical loss in K band and above is critical to designing acoustic resonators. Suspended HBARs provide a simple method of measuring metal thin film quality factor at high frequency.

REFERENCES

- [1] A. Hagelauer *et al.*, "From Microwave Acoustic Filters to Millimeter-Wave Operation and New Applications," *IEEE Journal of Microwaves*, vol. 3, no. 1, pp. 484–508, Dec. 2022, doi: 10.1109/JMW.2022.3226415.
- [2] Z. Schaffer, P. Simeoni, and G. Piazza, "33 GHz Overmoded Bulk Acoustic Resonator," *IEEE Microwave and Wireless Components Letters*, pp. 1–4, 2022, doi: 10.1109/LMWC.2022.3166682.
- [3] K. Ono, "A Comprehensive Report on Ultrasonic Attenuation of Engineering Materials, Including Metals, Ceramics, Polymers, Fiber-Reinforced Composites, Wood, and Rocks," *Applied Sciences* 2020, Vol. 10, Page 2230, vol. 10, no. 7, p. 2230, Mar. 2020, doi: 10.3390/APP10072230.
- [4] M. Ryzy et al., "Determining longitudinal and transverse elastic wave attenuation from zero-group-velocity Lamb waves in a pair of plates," J Acoust Soc Am, vol. 153, no. 4, pp. 2090–2090, Apr. 2023, doi: 10.1121/10.0017652.
- [5] C. Grünsteidl et al., "Measurement of the attenuation of elastic waves at GHz frequencies using resonant thickness modes," Appl Phys Lett, vol. 117, no. 16, p. 164102, Oct. 2020, doi: 10.1063/5.0026367/1078501.
- [6] N. Ishii, K. Kondo, M. Suzuki, and T. Yanagitani, "Mechanical transmission loss of the sole Bragg reflector by GHz pulse echo technique with thick SiO2delay line," *IEEE MTT-S International Conference on Microwave Acoustics and Mechanics, IC-MAM* 2022, pp. 82–85, 2022, doi: 10.1109/IC-MAM55200.2022.9855350.
- [7] B. P. Sorokin, N. O. Asafiev, G. M. Kvashnin, D. A. Scherbakov, S. A. Terentiev, and V. D. Blank, "Toward 40 GHz excitation of diamond-based HBAR," *Appl Phys Lett*, vol. 118, no. 8, p. 083501, Feb. 2021, doi: 10.1063/5.0038867.
- [8] N. Iwata, S. Kinoshita, and T. Yanagitani, "Extracting mechanical Q factor of the pure AlN, ScAlN, and ZnO films without etching substrate," *IEEE International Ultrasonics Symposium, IUS*, vol. 2020-September, Sep. 2020, doi: 10.1109/IUS46767.2020.9251667.
- [9] G. D. Mansfeld, S. G. Alekseev, and I. M. Kotelyansky, "Acoustic HBAR spectroscopy of metal (W, Ti, Mo, Al) thin films," Proceedings of the IEEE Ultrasonics Symposium, vol. 1, pp. 415– 418, 2001, doi: 10.1109/ULTSYM.2001.991652.
- [10] B. Sorokin, N. Asafiev, D. Yashin, N. Luparev, A. Golovanov, and K. Kravchuk, "Microwave Diamond-Based HBAR as a Highly Sensitive Sensor for Multiple Applications: Acoustic Attenuation in the Mo Film," Sensors 2023, Vol. 23, Page 4502, vol. 23, no. 9, p. 4502, May 2023, doi: 10.3390/S23094502.
- [11] G. M. Kvashnin, B. P. Sorokin, and A. S. Novoselov, "Peculiarities of energy trapping of the UHF elastic waves in diamond-based piezoelectric layered structure. I. Waveguide criterion," *Ultrasonics*, vol. 84, pp. 101–106, Mar. 2018, doi: 10.1016/j.ultras.2017.10.018.
- [12] G. M. Kvashnin and B. P. Sorokin, "Peculiarities of energy trapping of the UHF elastic waves in diamond-based piezoelectric layered structure. II. Lateral energy flow," *Ultrasonics*, vol. 111, p. 106311, Mar. 2021, doi: 10.1016/J.ULTRAS.2020.106311.
- [13] R. Lifshitz and M. Roukes, "Thermoelastic damping in micro- and nanomechanical systems," *Phys Rev B Condens Matter Mater Phys*, 2000, doi: 10.1103/PhysRevB.61.5600.
- [14] S. A. Chandorkar, M. Agarwal, R. Melamud, R. N. Candler, K. E. Goodson, and T. W. Kenny, "Limits of quality factor in bulk-mode micromechanical resonators," in *Proceedings of the IEEE International Conference on Micro Electro Mechanical Systems (MEMS)*, 2008. doi: 10.1109/MEMSYS.2008.4443596.
- [15] T. Grabec, M. Ryzy, P. Sedlák, and I. A. Veres, "Grain-boundary Scattering of Surface Acoustic Waves: Experiment and Simulation".
- [16] S. R. Bowden, "Optimization of Ion Beam Etch Sidewall Angle in Mo and Cr Films".